Geothermometry and geobarometry in epizonal granitic intrusions: a comparison of iron-titanium oxides and coexisting feldspars

JAMES A. WHITNEY AND J. C. STORMER, JR.

Department of Geology, University of Georgia
Athens, Georgia 30602

Abstract

Epizonal granites and quartz syenites from the White Mountain magma series, North Conway, New Hampshire, contain two feldspars, quartz, olivine, magnetite, ilmenite, biotite, clinopyroxene, and amphibole. The iron–titanium oxides from associated rhyolitic volcanic rocks yield extrusion temperatures of 1000 to 1050°C at an f_{O_2} of 10^{-11} bars. Those from the epizonal plutons yield temperatures of 650 to 700°C and an f_{O_2} of 10^{-18} bars, suggesting that the oxides reequilibrate during cooling to the solidus. These values agree with the f_{O_2}–T curves derived from the olivine–quartz–magnetite assemblages. The albite distribution between plagioclase and alkali feldspar yields temperatures above 1000°C for the volcanic rocks, 700 to 1000°C for the quartz syenite, and 650 to 700°C for the granite, suggesting that the feldspars record a more extensive portion of the crystallization history, but in general agree with the oxide temperatures. The biotite compositions suggest rather low values of f_{H_2O} during terminal crystallization (400 to 800 bars), but significant concentrations of chlorine and fluorine make this a maximum estimate. The low initial water content of the parent magma accounts for the high temperature of initial crystallization.

Introduction

The distribution of $NaAlSi_3O_8$ between two coexisting feldspars has long been recognized as a potentially valuable geothermometric tool. Since Barth (1934) proposed such a technique, it has been thoroughly discussed and a number of modifications proposed (Barth, 1951, 1956, 1962, 1970; Dunham, 1971; Orville, 1962; Perchuck and Ryabchikov, 1968). Recently, Stormer (1975) has proposed a model based on modern feldspar thermodynamic data. This model considers the effects of pressure, as well as non-ideality in alkali feldspars, on $NaAlSi_3O_8$ distribution. Before the proposed model may be accepted as a workable geologic tool, it must be tested in a variety of geologic settings. The current report is one in a series of such tests (Whitney *et al.*, 1975; Stormer and Whitney, 1975) and is a comparison of the geothermometric histories obtained from coexisting feldspars with those recorded by coexisting iron–titanium oxide solid solutions (Buddington and Lindsley, 1964) in epizonal granitic intrusions and related volcanic rocks.

Materials studied

During petrologic and geochemical study of a portion of the White Mountain Magma series within the North Conway quadrangle, New Hampshire, several lithologies were encountered which afforded an opportunity to compare the previously mentioned geothermometric techniques.

The White Mountain batholith was used by Buddington (1959) as an example of an epizonal intrusive complex. The occurrence of included blocks of contemporaneous volcanic rocks suggests a maximum depth at time of intrusion of a few kilometers. It therefore appears to be an ideal locale for the study of the application of modern geothermometric tools in the epizonal environment.

The North Conway quadrangle, first mapped in detail by Billings (1928), contains a portion of the White Mountain batholith, here composed of a series of coalesced alkalic plutons ranging in composition from syenite to granite. These bodies are Jurassic in age (Foland *et al.,* 1971; Armstrong and Stump, 1971) and have intruded igneous and regional meta-

morphic rocks of middle Ordovician to Devonian age. Within the batholith, isolated occurrences of the related Moat Mountain volcanic rocks are found, surrounded and intruded by the Conway granite and Albany quartz syenite. The quartz syenite forms numerous ring-dike structures within the White Mountain plutonic complex (Billings, 1928, 1956; Kingsley, 1931). These ring-dike structures, in conjunction with enclosed blocks of Moat Mountain volcanic rocks, have been interpreted as the remnants of caldera subsidence and may represent the remains of old

volcanic centers (Chapman, 1968). The Conway Granite intrudes both the Moat Mountain and the Albany formations, and is rather heterogeneous in this region, being composed of biotite, biotite–hornblende, and hornblende granites, with fayalitic olivine and calcic pyroxene being present in some lithologies.

Samples of the Albany quartz syenite and a hornblende granite member of the Conway granite contain fayalitic olivine, clinopyroxene, hornblende, biotite, magnetite, ilmenite, plagioclase, alkali feld-
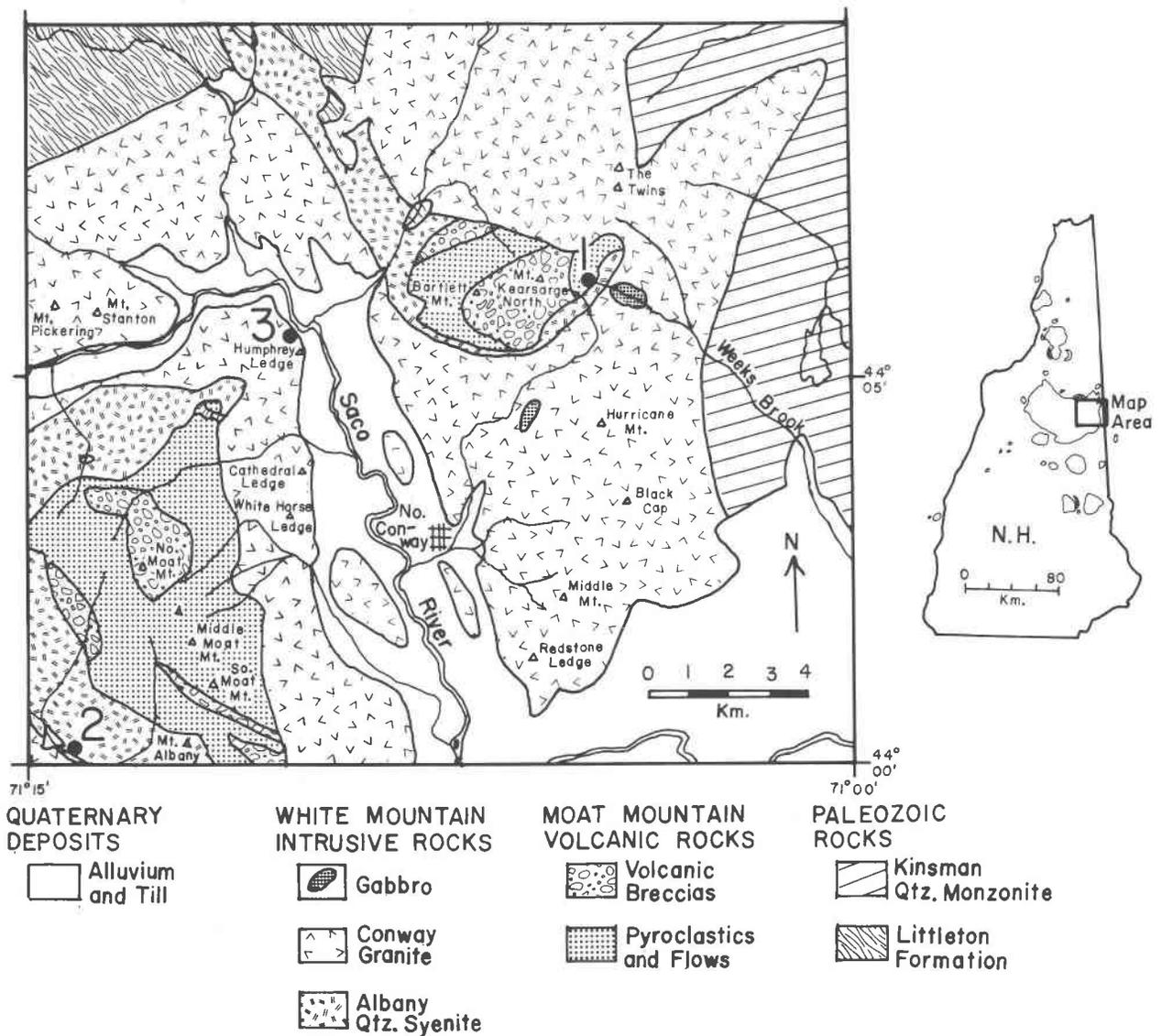
FIG. 1. Bedrock geology of a portion of the North Conway quadrangle, New Hampshire. Geology after Billings (1928). Sample locations: 1. Quartz trachyte flow, member of the Moat Mountain volcanics; 2. Albany quartz syenite; 3. Hornblende and fayalite-bearing member of the Conway granite.

spar microperthite, and quartz as major constituents. Two representative lithologies were chosen for detailed study (see Fig. 1 for sample localities). A sample of a volcanic flow from the Moat Mountain volcanic rocks, exposed on the southeast side of Mt. Kearsarge North, which contains phenocrysts of two feldspars, magnetite, and ilmenite was also selected for study.

Quartz trachyte flow

The volcanic sample was taken from the base of the Moat Mountain formation exposed in a stream valley of Weeks Brook, about 200 feet above the contact with the Albany quartz syenite. The majority of the Moat Mountain volcanic lithologies appear to have been tuffs, welded tuffs, or volcanic breccias (Noble and Billings, 1967). The sample chosen, however, is composed of abundant, euhedral alkali feldspar and quartz phenocrysts set in a homogeneous, dark grey, aphanitic groundmass. It is homogeneous with undeformed phenocrysts, a homogeneous groundmass, and contains no abundant clasts or inclusions. It thus appears to be a thin volcanic flow or very shallow intrusive. If the extensive volcanic breccia covering Mt. Kearsarge North is an old volcanic center, then this unit could represent a small obsidian flow from that source. This flow is overlain by a series of pyroclastic rocks rich in quartz, and appears to have been subsequently intruded by a phase of the Albany formation.

Upon microscopic examination, the alkali feldspar is found to be homogeneous, with a few traces of perthitic exsolution. Optically, it has a moderate negative $2V$ and appears to be orthoclase of an intermediate composition. Plagioclase phenocrysts are not common, and the outer portions often show some sericitization, which must be avoided during chemical analysis. Estimates of composition using flat stage techniques ranged from An_{40} to An_{50} with little indication of compositional zonation.

Quartz phenocrysts are commonly embayed, but good bipyramidal terminations are still recognizable. Microphenocrysts include ferrohastingsite-rich hornblende, ilmenite, and rare magnetite. One large, apparently embayed, crystal of pyrite was also observed.

The groundmass is composed of a dense, aphanitic intergrowth of ferrohastingsite-rich hornblende, alkali feldspar, plagioclase(?), and ilmenite with minor quartz. Accessories include apatite and zircon. Sphene is found as fine-grained, polycrystalline rims on some ilmenite.

A few small inclusions of an amphibolite composed of hornblende, ilmenite, and apatite are found (autoliths?) along with fragments of other volcanic rocks.

Chemically, the rock as a whole (Table 1, column 1) could be termed a rhyolite, although it contains only 12 percent normative quartz. The groundmass, however, contains only about 1 percent normative quartz and would better be termed a trachyte. It will here be termed a "quartz trachyte" indicating a trachytic melt containing quartz phenocrysts, with a bulk composition transitional between trachyte and rhyolite.

Albany quartz syenite

The sample of the Albany formation was taken from a road cut along the Swift River, just north of the covered bridge on Dugway road at its intersection with the Kankamungas highway. It is porphyritic with alkali feldspar phenocrysts set in a medium-gray, fine-grained groundmass. It is somewhat variable in composition from quartz syenite to granite.

TABLE 1. Chemical analyses

	QUARTZ TRACHYTE		QUARTZ SYENITE		GRANITE
	Whole Rock	Ground Mass	Whole Rock	Ground Mass	
SiO_2	65.9	56.7	67.2	65.3	70.2
TiO_2	0.93	1.46	0.51	0.66	0.25
Al_2O_3	14.6	16.4	13.9	13.5	14.2
Fe_2O_3	2.05	1.21	1.09	0.73	0.74
FeO	3.04	6.16	3.29	4.65	2.39
MnO	0.18	0.34	0.15	0.20	0.13
MgO	1.00	1.89	0.30	0.42	0.05
CaO	2.22	3.51	1.53	1.93	1.15
Na_2O	4.65	4.26	3.95	3.88	4.17
K_2O	5.50	4.67	5.42	4.59	5.78
H_2O^+	0.76	1.47	0.30	0.44	0.19
H_2O^-	0.09	0.15	0.08	0.11	0.09
Total	100.92	98.22	97.72	96.41	99.34
Normative Equivalent					
Q	12.1	1.0	18.4	17.9	20.2
Or	32.5	27.6	32.0	27.1	34.2
Ab	39.4	36.1	33.4	32.8	35.3
An	2.7	11.8	4.2	5.9	3.0
$CaSiO_3$	3.5	2.3	1.4	1.6	1.2
$MgSiO_3$	2.5	4.8	0.7	1.0	0.1
$FeSiO_3$	2.7	8.5	4.5	7.2	3.6
Mt	3.0	1.8	1.6	1.1	1.1
Il	1.8	2.8	1.0	1.3	0.5
Differentiation Index	84.0	64.7	83.8	77.8	89.7

Note: All analyses by XRF except: MgO and Na_2O, atomic absorption; FeO, diphenylamine titration; total H_2O, water emission on fusion in Penfield tube.

The sample chosen contains about 15 percent modal quartz and should therefore be called a granite.

Microscopically, the alkali feldspar is strongly perthitic. The distribution of albite lamellae is normally quite uniform, except at the very edge of a grain. In a few cases, however, large patches of albite are observed which might be the product of replacement. The optical orientation of the host feldspar, however, appears to be perpendicular to that found in phenocrysts having fine lamellae, suggesting that these patches may be caused by sectioning nearly parallel to the lamellae. The homogeneity in composition of the majority of the phenocrysts suggests that they represent initial igneous feldspar compositions which have undergone exsolution with some possible $NaAlSi_3O_8$ loss from the edge of the grains.

In addition to the obvious feldspar phenocrysts, almost every thin-section contains one or two large, highly rounded grains of quartz. These sparse but ubiquitous quartz phenocrysts are probably early phenocrysts which were partially resorbed during intrusion.

The groundmass is composed of plagioclase, quartz, and a variety of mafic minerals. The plagioclase is commonly euhedral, with strong normal zoning. Flat-stage optical techniques yielded compositions ranging from An_{45} to An_{25}. Although the plagioclase does not form phenocrysts, it appears to have coexisted with alkali feldspar over a substantial portion of the crystallization history. Euhedral plagioclase grains are found included throughout most of the alkali feldspar. The composition of these inclusions found in the core of alkali feldspar phenocrysts corresponds to that of interior zones of the free plagioclase. Those found in the outer portions of the phenocrysts are commonly more sodic. Thus it appears that the cores of the two feldspars formed in equilibrium with one another, and they coexisted over most of the crystallization history. The disparity in size between alkali feldspar and plagioclase is probably caused by differences in nucleation and growth rates rather than differences in the length of time taken for crystallization.

The majority of the mafic minerals are found in clots composed of minor calcic clinopyroxene and fayalitic olivine, overgrown with ferrohastingsite-rich hornblende and iron-rich biotite. Euhedral magnetite and ilmenite grains up to 1 mm in size are common in these clots. The ilmenite, and rarely magnetite, are also found included within feldspars and as free crystals. Olivine, clinopyroxene, ilmenite, and magnetite appear to have been early phases with hornblende subsequently nucleating on the preexisting mafic minerals, and biotite forming at the very end of magmatic crystallization.

Accessory minerals include apatite and zircon,

TABLE 2. Chemical analyses of magnetite and ilmenite

| | QUARTZ TRACHYTE | | | | ALBANY QUARTZ SYENITE | | | | | | | CONWAY GRANITE | | | | | |
| | Mag. | Ilmenite | | | Magnetite | | | Ilmenite | | | | Magnetite | | Ilmenite | | | |
	1.	2.	3.	4.	5.	6.	7.	8.	9.	10.	11.	12.	13.	14.	15.	16.	17.
SiO_2	0.3	0.1	0.1	0.1	<0.05	<0.05	0.2	0.5	<0.05	0.2	<0.05	0.1	0.1	0.1	<0.05	0.1	0.1
TiO_2	23.7	49.1	49.4	49.3	10.3	10.1	10.4	49.4	51.9	48.9	48.7	7.1	8.5	48.9	48.8	46.9	44.9
Nb_2O_3	0.2	1.5	0.7	2.0	<0.05	<0.05	<0.05	0.3	0.2	1.9	2.0	<0.05	<0.05	1.4	1.8	2.5	4.0
Fe_2O_3 FeO }	66.7[1]	41.4[1]	45.2[1]	39.4[1]	84.4[1]	82.4[1]	82.2[1]	47.0[1]	47.5[1]	47.0[1]	47.4[1]	84.0[1]	82.5[1]	46.4[1]	46.4[1]	47.7[1]	47.5[1]
MnO	0.9	7.3	4.4	9.8	0.4	0.4	0.8	1.8	1.6	1.7	1.9	0.5	0.5	2.7	2.9	1.7	2.2
MgO	<0.05	<0.05	<0.05	<0.05	<0.05	<0.05	<0.05	<0.05	<0.05	<0.05	<0.05	<0.05	<0.05	<0.05	<0.05	<0.05	<0.05
CaO	0.03	0.02	0.02	0.12	0.01	<0.01	<0.01	0.01	0.01	<0.01	<0.01	0.02	0.02	0.02	0.02	0.03	<0.01
Total	91.8	99.4	99.8	100.7	95.2	93.0	93.6	99.0	101.2	99.7	100.0	91.7	91.6	99.5	99.9	98.9	98.7
Calculated																	
Fe_2O_3	18.0	5.0	5.9	5.6	49.0	47.9	47.3	4.1	2.8	5.0	6.2	53.1	49.9	5.7	5.8	7.9	10.3
FeO	50.5	36.9	39.9	34.4	40.3	39.3	39.6	43.3	45.0	42.5	41.8	36.2	37.6	41.2	41.2	40.6	38.2
Total[2]	93.6	99.9	100.4	101.3	100.1	97.8	98.3	99.4	101.5	100.2	100.6	97.0	96.6	100.0	100.5	99.7	99.7
$\frac{Usp \times 100}{Usp + Mt}$	71.0				29.1	29.1	29.5					20.4	24.8				
$\frac{Hem \times 100}{Hem + Ilm}$		5.8	6.3	6.7				4.1	2.7	5.1	6.3			5.9	5.9	8.1	10.8

[1] Total iron as FeO.

[2] Totals of analyses corrected for excess O_2 combined with ferric iron.

Note: Analyses nos. 4 and 11 are from grains included in hornblende, while analyses 7, 10, and 16 are from grains included in feldspar. Analysis number 17 is from a large, rounded ilmenite grain.

with occasional fluorite and monazite. A dark brown iddingsite alteration is commonly associated with the olivine.

The chemical composition of the rock as a whole (Table 1, column 3) is similar to the quartz trachyte, but is slightly depleted in sodium, calcium, and magnesium. The groundmass (Table 1, column 4) is similar in composition to that of the whole rock, and both contain about 18 percent normative quartz.

Conway granite

The sample of the Conway granite studied is a hornblende-bearing phase collected from a road cut on the northeast side of Humphrey's Ledge. It is medium-grained, light yellowish-gray, hypidiomorphic-granular rock composed of alkali feldspar, plagioclase, and quartz with a variety of mafic minerals.

Microscopically, the alkali feldspar is strongly perthitic with albite lamellae evenly distributed throughout the grains. The plagioclase is about An_{10} in composition with slight normal zoning. A few euhedral inclusions of plagioclase are found within alkali feldspar.

A number of the mafic minerals are found in clots containing clinopyroxene and fayalitic olivine with overgrowths of ferrohastingsite-rich hornblende and minor iron-rich biotite. Euhedral crystals of magnetite and ilmenite are common, both in clots and included in feldspar. As in the Albany sample, olivine, clinopyroxene, ilmenite, and magnetite appear to be early phases with hornblende and lastly biotite forming during cooling.

Several large (up to 2mm), rounded, free grains of ilmenite were found which differed chemically from the majority of the grains. These appeared anomalous both in appearance and chemistry and may have been inherited from some other source.

Common accessories include apatite, zircon, monazite, allanite, and fluorite. A dark brown iddingsite alteration is again found associated with the olivine.

Chemically, (Table 1, column 5) the granite is similar to the Albany sample, but is somewhat richer in normative quartz and feldspar and poorer in mafic constituents.

Iron–titanium oxides

Temperature and oxygen fugacities were determined using the iron–titanium oxide geothermometer (Buddington and Lindsley, 1964). This technique depends upon an equilibrium of the ulvöspinel and magnetite components in "magnetite" solid solution with the ilmenite and hematite components of the "ilmenite" solid solution.

Analytic procedure

Major-element analyses of cubic and rhombohedral iron–titanium oxides were done on a MAC 400S electron microprobe employing three wavelength-dispersive crystal spectrometers. In order to identify all major elements, X-ray emission spectra were obtained with an energy-dispersive system with a lithium-drifted silicon scintillation detector and a multichannel analyzer providing 152 eV FWHM resolution at MnK_α. Standards used included synthetic Fe_3O_4 and TiO_2. All analyses were corrected for matrix effects using the technique of Bence and Albee (1968) and the correction factors of Albee and Ray (1970). Results on selected grains are summarized in Table 2. All grains analyzed were first examined under reflected light to assure homogeneity. A number of titaniferous magnetite grains show small amounts of ilmenite exsolution near their outer edge, presumably due to oxidation. Such regions were avoided during analysis. All grains analyzed proved to be chemically homogeneous, with no statistically significant variation in composition being observed over the optically homogeneous portions of the grains.

Buddington and Lindsley (1964) calibrated the magnetite–ilmenite geothermometer (Fig. 2) for a system containing only iron, titanium, and oxygen, and it is not clear how the other components (such as manganese and niobium) should be treated. In addition, there is some ambiguity as to the best procedure for recalculating microprobe analyses, in which only total iron can be determined.

For this work, we have adopted the procedure given by Carmichael (1967) for recalculation. After calculating the various mineral components (Nb as Nb^{+3} analogs of magnetite and hematite, and Mn^{+2} and Mg^{+2} as analogs of ulvöspinel and ilmenite), the molar ratio of *only* $Fe_2O_3/(FeTiO_3+Fe_2O_3)$ and $Fe_3O_4/(Fe_3O_4+Fe_2TiO_4)$ were used to establish the temperature and oxygen fugacity on Buddington and Lindsley's curves. This in effect treats the extraneous components as inert diluents in the mineral solid solutions which in the absence of more complete information seems the most reasonable procedure thermodynamically.

Analytical results

In the volcanic sample, ilmenite is by far the dominant iron–titanium oxide. Only one small microphenocryst of magnetite was found in the polished
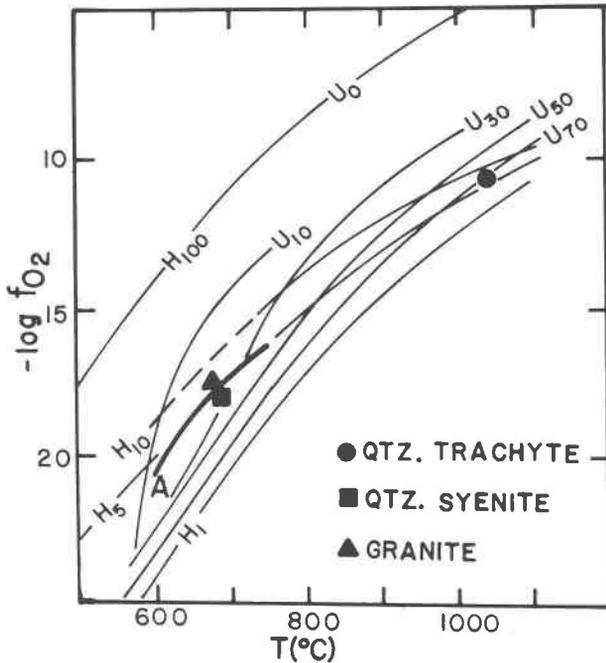
FIG. 2. F_{O_2}–T diagram for the iron-titanium oxides. Calibration curves represent the hematite content of ilmenite solid solutions and the ulvöspinel content of magnetic solid solutions as given by Buddington and Lindsley. Filled symbols represent the compositions of coexisting phases from the various lithologies. Curve A is the f_{O_2}–T conditions for the Albany quartz syenite and Conway granite samples as defined by the assemblage olivine–quartz–magnetite.

sections studied, along with several apparent overgrowths of magnetite on ilmenite. When plotted against the determinative curves of Buddington and Lindsley (Fig. 2), the coexisting microphenocrysts indicate an equilibration temperature of 1040°C at an f_{O_2} of $10^{-10.7}$ bars. Such temperatures are quite high compared to those commonly suggested for trachytic or rhyolitic magmas (see for example values listed by Carmichael et al., 1974, p. 7). The f_{O_2}–T conditions do however fall close to the curve defined by the assemblage quartz–fayalite–magnetite. Such conditions are thought to be reasonable for a variety of magmatic systems (Carmichael, 1967).

Both oxide phases are common in the two intrusive lithologies. Within each sample most grains are similar in composition, with one notable exception. The large, rounded ilmenite grains encountered within the granite sample are strikingly different in that they contain about 4 percent niobium oxide (calculated as Nb_2O_3). These grains were not found in direct association with magnetite, and so for the current study were not used in defining the f_{O_2}–T conditions.

When plotted against the curves of Buddington and Lindsley, the oxides from the Albany quartz syenite yield equilibration temperatures of ~690°C at an oxygen fugacity of 10^{-18} bars. The values obtained for the granite sample are similar, ~680°C and $10^{-17.7}$ bars. These temperature values are close to the solidus for granitic rocks at low pressures (Tuttle and Bowen, 1958). It would therefore appear that the oxides in these epizonal plutons have reequilibrated during crystallization at least as long as a silicate liquid phase was present, but ceased reaction at temperatures near the solidus. In both cases, the f_{O_2}–T conditions fall close to the buffer curve defined by the assemblage quartz–fayalite–magnetite.

Comparison with the assemblage quartz–olivine–magnetite

The coexistence of quartz, olivine, and magnetite in the Albany quartz syenite and Conway granite samples allows another check on the f_{O_2}–T conditions of equilibration. The reaction between iron end-members is expressed by the reaction

$$3\ SiO_2 + 2\ Fe_3O_4 = 6\ Fe(SiO_4)_{1/2} + O_2$$
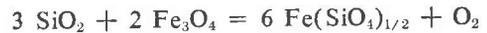
$$\exp -\left(\frac{\Delta G^\circ}{RT}\right) = K_f = \left(\frac{f_{O_2} \cdot a_{fa}^6}{a_{mt}^2 \cdot a_q^3}\right).$$

Assuming that the activity of quartz is 1, the activities of fayalite in olivine and magnetite in magnetite solid solution may be approximated by mole fraction and rearranging to logarithmic form, the equilibrium relationship of this reaction becomes.

$$\log f_{O_2} = -\left(\frac{\Delta G^\circ}{RT}\right) - 6 \log X_{fa} + 2 \log X_{mt}$$

from which f_{O_2}–T curves may be calculated.

The olivine in each sample was analyzed using analytic conditions similar to those employed for the iron–titanium oxides, with analyzed olivine and synthetic Fe_3O_4 standards. The resulting olivine compositions, corrected for matrix effects as before, are summarized in Table 3.

The f_{O_2}–T curves calculated for the above assemblages (Fig. 2) agree closely with the values obtained from the iron–titanium oxides. This correspondence further confirms that the determined conditions represent equilibrium, and that the oxide compositions have not been subsequently changed by alteration or oxidation.

Equilibration temperatures of coexisting feldspars

One of the principal objectives of this work is to establish the applicability of a two-feldspar geother-

TABLE 3. Chemical analyses of olivine

	ALBANY QTZ. SYENITE			CONWAY GRANITE			
	1.	2.	3.	4.	5.	6.	7.
SiO$_2$	27.7	28.1	27.2	28.1	27.3	27.9	27.3
Fe$_2$O$_3$ FeO	64.9*	65.3*	65.0*	63.6*	64.7*	65.4*	65.6*
MnO	2.6	2.8	2.6	3.8	3.8	3.8	3.8
MgO	1.2	0.7	1.0	0.06	0.05	0.06	0.05
CaO	0.1	0.1	0.1	0.1	0.2	0.1	0.1
	96.5	97.0	95.9	95.7	96.1	97.4	96.8
Number of Ions Based on 8 (0).							
Si	0.97	0.98	0.97	1.00	0.97	0.98	0.97
Fe	1.91	1.91	1.93	1.88	1.93	1.92	1.95
Mn	0.08	0.08	0.08	0.12	0.12	0.11	0.12
Mg	0.06	0.04	0.05	0.00	0.00	0.00	0.00
Ca	0.00	0.00	0.00	0.00	0.00	0.00	0.00

*Total iron as FeO.

mometer, based on the distribution of albite component between plagioclase and alkali feldspar (Stormer, 1975), to epizonal granitic rocks. By treating the two feldspars as essentially binary solutions, and applying modern thermodynamic data for binary feldspar solutions, it was possible to derive an analytic expression relating the albite content of coexisting feldspars to temperature and pressure. Determinative curves (see Fig. 3) have been previously shown to give reasonable agreement with available ternary feldspar experimental data and with that from volcanic rocks (Stormer, 1975). With careful petrographic interpretation, the geothermometer gives consistent and useful informatin for mesozonal granites (Whitney *et al.*, 1975) and granulite facies metamorphic rocks (Stormer and Whitney, 1975).

Analytic procedure

The mole fraction of NaAlSi$_3$O$_8$ in coexisting feldspars was determined in all samples by analysis for Na, K, and Ca on the electron microprobe using wavelength-dispersive crystal spectrometers. Energy-dispersive X-ray spectra were again used to identify all major elements present. Small amounts of barium are present, but quantities are insufficient to affect the current use of the data. An excitation potential of 15 kV was used and the sample current set so that volatilization of sodium from a pure albite standard was undetectable across a two-minute period. Each analysis represents the average of a minimum of five 20 second counts on a sample. Analyzed natural feldspars were used as standards to minimize matrix ef-

fects, and all analyses were corrected as before using the factors listed by Albee and Ray (1970).

Determining the average composition of microperthite in the plutonic samples presented an analytic problem. Grains were chosen that showed fine homogeneously-distributed lamellae. The electron beam was than defocused to give a broad, about 30 micron, beam. Bulk analysis of inhomogeneous material with homogeneous standards by broad-beam techniques can lead to errors from matrix effects. But, in the case of perthitic lamellae in alkali feldspar, these effects will be similar in each phase and in the standards, and therefore errors should be insignificant. A series of about 20 to 25, 20-second counts were taken from contiguous areas covering a portion of the grain. These values were averaged to give a representative analysis for the whole area. Care was taken to avoid the very edges of grains, where albite had apparently been lost from the grain on exsolution. Plagioclase inclusions and large patches of NaAlSi$_3$O$_8$ which could have been the product of replacement were also avoided. The resulting mole fractions of NaAlSi$_3$O$_8$ are represented in Figure 3, with representative analyses being listed in Table 4.
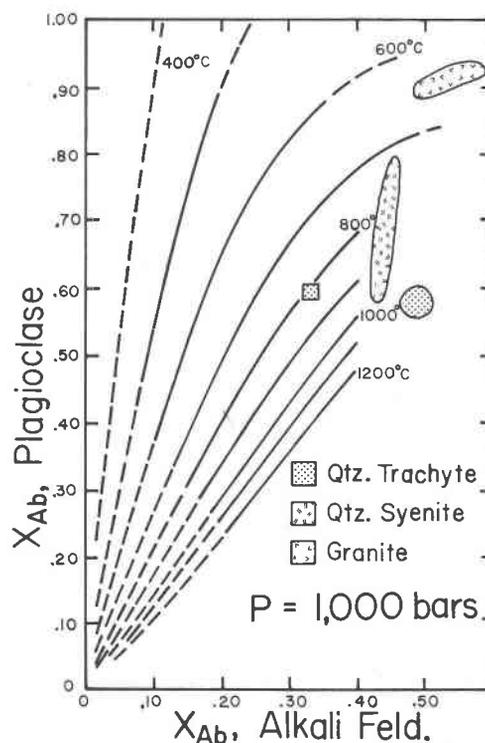
FIG. 3. Albite distribution between coexisting feldspars. Temperature calibration curves from Stormer (1975). Feldspar compositions determined as described in the text.

TABLE 4. Representative feldspar analyses

PHASE		Ab	Or	An	Total	Ab
		WEIGHT %				MOLE %
QUARTZ TRACHYTE						
Plagioclase		59.2	2.5	35.7	97.4	62.2
		57.0	3.4	39.5	99.9	58.6
		53.4	3.0	42.9	99.3	55.3
Alkali Feldspar		45.8	50.3	1.3	97.6	48.4
		49.7	50.4	2.0	102.1	50.2
		49.5	45.4	1.4	96.4	52.8
	Rim	31.8	61.4	2.3	94.5	35.0
QUARTZ SYENITE						
Plagioclase	Core	56.7	0.3	41.2	98.2	59.2
	Core	56.3	0.1	35.9	92.3	62.4
	Interior Zone	60.9	0.3	36.8	96.0	64.8
	Outer Margin	72.5	0.6	26.2	99.3	74.2
	Outer Margin	73.8	0.4	24.1	98.3	76.2
	Outer Margin	79.1	0.7	17.7	97.5	82.0
Alkali Feldspar		42.5	51.9	1.0	95.4	46.0
		41.9	60.2	0.6	102.7	42.2
		44.7	53.7	0.9	98.3	47.0
GRANITE						
Plagioclase		89.1	1.1	7.5	97.7	91.7
		91.2	1.3	6.4	98.9	92.6
		91.1	1.6	8.1	100.8	90.9
		92.7	3.0	6.4	102.1	91.3
	Rim	92.9	1.0	6.7	100.6	92.7
Alkali Feldspar		47.9	50.9	0.8	97.7	50.5
		48.8	51.9	0.8	101.5	49.6
		50.5	48.0	0.9	99.4	52.3
	Outer Margin	49.7	50.9	0.8	101.4	50.5
	Outer Margin	50.6	49.9	1.0	100.6	51.8
	Interstitial	57.1	40.7	1.1	98.9	59.2

Interpretation of results

The current model of $NaAlSi_3O_8$ distribution requires that the confining pressure at the time of equilibration be estimated. Since the intrusive environment is epizonal, and throught to have been only a few kilometers deep, a pressure of one kilobar was used.

Such an assumed pressure is reasonable for the intrusive rocks, but the pressure at which feldspar phenocrysts in the volcanics equilibrated is not known. Feldspars from the volcanic quartz syenite yield temperatures of about 1000°C at one kilobar confining pressure. These values are in excellent agreement with temperatures obtained from the iron–titanium oxides (Table 5). Increasing the assumed pressure increases the temperature estimate by about 20°C/kbar. It therefore appears that the feldspar phenocrysts must have equilibrated at fairly low pressures, since they would otherwise yield too high a temperature. A few grains of alkali feldspar have rims which have lower sodium contents, yielding a lower temperature of about 810°C. These rims may have

formed during crystallization of the flow, or may represent some loss of sodium from the edge of the grain during subsequent events.

The feldspars from the Albany quartz syenite suggest a more complex cooling history. The plagioclase shows strong normal zonation from An_{40} in the cores to An_{20} at the edges. The alkali feldspar does not show strong zonation, but perthite exsolution may have masked small initial variations. Euhedral inclusions of plagioclase within alkali feldspar suggest that the two feldspars coexisted throughout most of the crystallization history. Equilibration temperatures obtained, assuming a confining pressure of one kilobar, range from about 1000°C for the cores to around 700°C for the outer margins. The lowest crystallization temperatures obtained are in excellent agreement with the iron–titanium oxide data (Table 5), and correspond to the expected solidus temperature for this material. The feldspars, however, appear to record a much more extensive portion of the crystallization history than do the oxide phases. Apparently the oxide minerals reequilibrate during crystallization, while the feldspars do not.

The feldspars from the Conway granite sample are less strongly zoned, with plagioclase compositions of around An_8. Temperatures calculated from various pairs, assuming a one kilobar confining pressure, give a temperature of 650 to 700°C. These values are again consistent with the iron–titanium oxide data (Table 5), and suggest that most of the feldspar crystallization occurred over a small temperature interval.

Water fugacity and its effects on crystallization temperatures

As previously noted, the temperatures for oxide equilibration and feldspar crystallization in the volcanic samples and for the first feldspar crystallization in the Albany quartz syenite are around 1000°C, which is very high for crystallization from a granitic composition. Comparison of the quartz syenite with the synthetic data of Whitney (1975) suggests that feldspar could start crystallizing at such high temper-

TABLE 5. Comparison of temperature and f_{O_2} from various methods

Lithology	T from Feldspars	T from Fe-Ti Oxides	f_{O_2} from Fe-Ti Oxides	f_{O_2} from Q-Ol-Mag at T
Qtz. Trachyte	1095-810°C	1040°C	$10^{-10.7}$ bars	--------
Qtz. Syenite	1065-710°C	690°C	10^{-18} bars	$10^{-17.8}$ bars
Granite	700-650°C	680°C	$10^{-17.7}$ bars	$10^{-18.1}$ bars

atures only if the activity of water in the magma was quite low.

The occurrence of biotite in an assemblage containing alkali feldspar and magnetite allows the water fugacity to be estimated through the reaction:

$$KFe_3AlSi_3O_{10}(OH)_2 + \tfrac{1}{2}O_2$$
$$= KAlSi_3O_8 + Fe_3O_4 + H_2O$$
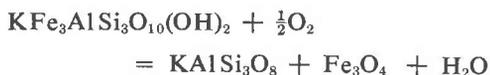
$$\exp\ -\left(\frac{\Delta G_0}{RT}\right) = K = \frac{a_{or} \cdot a_{mt} \cdot f_{H_2O}}{a_{ann} \cdot f_{O_2}^{1/2}}$$

(Wones and Eugster, 1965). Since the fugacity of oxygen and the approximate temperature are known for the final crystallization of the intrusive rocks, an approximation may be made to the water fugacity in the late stage melts using the equation of Wones and Eugster (1965) as modified by Wones (1972).

Chemical analyses of the biotites were determined by microprobe analysis under conditions similar to those described previously. Since the biotite standards used were nearly identical to the unknown samples, correction for matrix effects were omitted. The compositions obtained are listed in Table 6. Structural formulas were calculated assuming all the iron to be in the ferrous state, and the hydroxyl sites to be filled with $(OH,F,Cl)^-$. The activity of magnetite was assumed to be equal to mole fraction, and the activity of potassium feldspar was calculated from the mole fraction in alkali feldspar according to the Thompson and Waldbaum (1969), and Waldbaum and Thompson (1969) model.

The values for water fugacity obtained were 300 to 400 bars in the quartz syenite and up to 800 bars in the granite. These, however, are maximum estimates. The fluorine analyses are only approximate as the counting statistics are poor for such low-energy radiations. The biotite in both samples appears to have formed very late in the crystallization history. The water fugacity calculated is therefore that obtained at the end of crystallization history. During the crystallization of the quartz syenite, the water activity in the melt would increase as anhydrous phases were removed. The initial water fugacity was probably much less, and the water content of the original melt was probably not greater than 0.5 percent.

The quartz syenite composition is very similar to the synthetic adamellite (R4) composition studied by Whitney (1975). Two-kilobar data for that composition suggests that crystallization of two coexisting feldspars would occur at temperatures of about 1000°C at such low water content. Thus, the high initial crystallization temperatures obtained from the

TABLE 6. Chemical analyses of biotites

	ALBANY QUARTZ SYENITE		CONWAY GRANITE	
SiO$_2$	35.5	36.6	32.9	33.3
TiO$_2$	2.9	0.8	3.6	1.8
Al$_2$O$_3$	8.4	9.1	9.6	12.4
Fe$_2$O$_3$ / FeO	36.1[1]	33.4[1]	41.2[1]	40.3[1]
MnO	0.3	0.4	0.5	0.7
MgO	4.3	6.6	0.2	0.1
Na$_2$O[2]	(0.1)	(0.1)	(0.3)	(0.3)
K$_2$O	8.7	8.9	8.7	8.3
Cl	0.2	0.2	0.4	1.0
F	(0.5)	(0.5)	(1.)	(2.)
Total	97.0	96.6	98.4	100.2
O ≡ (F,Cl)	- 0.3	- 0.3	- 0.5	- 1.1
H$_2$O[3]	3.3	3.8	2.8	2.3
Total	100.0	100.1	100.7	101.4

Number of Ions Based on 10 (O) and 2 (OH, F, Cl) Sites.

	Albany QS		Albany QS		Conway		Conway	
Si	2.94 } 3.76		2.99 } 3.87		2.80 } 3.76		2.79 } 4.00	
Al	0.82		0.88		0.96		1.21	
Al	--		--		--		--	
Ti	0.18		0.05		0.23		0.12	
Fe	2.50 } 3.23		2.29 } 3.17		2.93 } 3.22		2.83 } 3.02	
Mn	0.02		0.02		0.04		0.05	
Mg	0.53		0.81		0.02		0.01	
Na	0.01 } 0.93		0.01 } 0.94		0.05 } 1.00		0.05 } 0.93	
K	0.92		0.93		0.95		0.89	
Cl	0.03		0.03		0.05		0.14	
F	0.13 } 2.00		0.10 } 2.00		0.35 } 2.00		0.56 } 2.00	
OH	1.84		1.87		1.60		1.30	

[1] Total iron as FeO.

[2] Sodium determined by graphical analysis of energy dispersive X-ray emission spectra.

[3] Calculated assuming full occupancy of (OH) sites with OH, F, and Cl.

cores of the feldspars are consistent with synthetic data on similar compositions with these low water contents.

Summary and conclusions

The iron–titanium oxides and coexisting feldspars found in these epizonal and volcanic lithologies yield consistent thermal histories. The volcanic sample appears to have crystallized phenocrysts and microphenocrysts at temperatures of around 1000°C. The quartz syenite appears to have commenced crystallization at a similar temperature, but continued crystallization down to temperatures of around 700°C. The iron–titanium oxides reequilibrated during cooling, while the feldspars did not. The granite sample appears to have crystallized over a short temperature interval, with both geothermometers yielding the same result. This temperature corresponds to the lower temperatures from the quartz syenite.

In conclusion, the magmas now represented by the quartz trachyte and quartz syenite apparently originated at temperatures of 1000°C or more from a very dry source. The Albany formation subsequently underwent a long crystallization history in the epizonal environment as its temperature decreased to about 700°C. The granite sample studied would appear to be a late-stage fractionation product of this crystallization, with the solidification of this residual melt taking place over a narrow temperature range.

During this process, the water activity was presumably increasing steadily, but even in the late stages it was only a few hundred bars. Initial water contents of the magma probably did not exceed 0.5 weight percent or so.

The oxygen fugacity in the magma was dominantly controlled by the reaction of olivine, magnetite, and a silica-rich magma, possibly in the presence of quartz. The oxygen fugacity therefore appears to have closely followed the quartz–fayalite–magnetite buffer curve during cooling.

The two-feldspar geothermometer of Stormer (1975) appears to give satisfactory results in epizonal plutonic rocks, as long as careful petrographic observations are used to determine which phases may have been in equilibrium. In addition, some technique must be used to determine the average composition of perthitic feldspars. In the case of homogeneous microperthite, the technique of using a defocused electron microprobe beam seems to give reliable results.

The application of this refined tool in geothermometry should open the way for detailed consideration of the thermal history of feldspar crystallization in a variety of igneous occurrences.

Acknowledgments

References

ALBEE, A. L. AND L. RAY (1970) Correction factors for electron probe microanalysis of silicates, oxides, carbonates, phosphates, and sulfates. *Anal. Chem.* **42**, 1408–1414.

ARMSTRONG, R. L. AND E. STUMP (1971) Additional K–Ar dates, White Mountain magma series, New England. *Am. J. Sci.* **270**, 331–333.

BARTH, T. F. W. (1934) Polymorphic phenomena and crystal structure. *Am. J. Sci.* **5**, 273.

——— (1951) The feldspar geological thermometers. *Neues Jahrb. Mineral. Abhandl.* **82**, 143–154.

——— (1956) Studies in gneiss and granite. *Skrifter Norske Vidensk.-Akad. Oslo. I. Mat.-Naturv Klasse*, No. 1, 263–274.

——— (1962) The feldspar geologic thermometer. *Norsk. Geol. Tidsskr.* B. **42**, 330–339.

——— (1968) Additional data for the two-feldspar geothermometer. *Lithos*, **1**, 305–306.

BENCE, A. E. AND A. L. ALBEE (1968) Empirical correction factors for the electron microanalysis of silicates and oxides. *J. Geol.*, **76**, 382–403.

BILLINGS, M. P. (1928) The petrology of the North Conway quadrangle in the White Mountains of New Hampshire. *Proc. Am. Acad. Arts Sci.*, **63**, 67–137.

——— (1956) The geology of New Hampshire: Pt. II. Bedrock geology: *New Hampshire Plann. Dev. Comm. Miner. Resour. Surv.*, p. 1–203.

BUDDINGTON, A. F. (1959) Granite emplacement with special emphasis on North America. *Geol. Soc. Am. Bull.* **70**, 671–748.

——— AND D. H. LINDSLEY (1964) Iron-titanium oxide minerals and synthetic equivalents. *J. Petrol.* **5**, 310–357.

CARMICHAEL, I. S. E. (1967) The iron-titanium oxides of salic volcanic rocks and their associated ferromagnesian silicates. *Contrib. Mineral. Petrol.* **14**, 36–64.

———, F. J. TURNER AND J. VERHOOGEN (1974) *Igneous Petrology.* McGraw-Hill, New York, 739 p.

CHAPMAN, C. A. (1968) A comparison of the Maine coastal plutons and the magmatic central complexes of New Hampshire. In, Zen, White, and Hadley, Ed., *Studies of Appalachian Geology, Northern and Maritime.* John Wiley and Sons, New York, p. 385–396.

DUNHAM, A. C. (1971) The two-feldspar geothermometer. *Ann. Acad. Brazil Cienc.* **43**, 627–631.

FOLAND, K. A., A. W. QUINN AND B. J. GILETTI (1971) K–Ar and Rb–Sr Jurassic and Cretaceous ages for intrusives of the White Mountain Magma Series, Northern New England. *Am. J. Sci.* **270**, 321–330.

KINGSLEY, L. (1931) Cauldron-subsidence of the Ossipee Mountains, *Am. J. Sci.* **222**, 139–163.

NOBLE, D. C. AND M. P. BILLINGS (1967) Pyroclastic rocks of the White Mountain Magma series, New Hampshire. *Nature,* **216**, 906–907.

ORVILLE, P. M. (1962) Comments on the two-feldspar geothermometer. *Norsk Geol. Tidsskr.* **42**, 340–346.

PERCHUCK, L. L. AND I. D. RYABCHIKOV (1968) Mineral equilibria in the system nepheline–alkali feldspar–plagioclase and their petrological significance. *J. Petrol.* **9**, 123–167.

STORMER, J. C., JR. (1975) A practical two-feldspar geothermometer. *Am. Mineral.* **60**, 667–674.

——— AND J. A. WHITNEY (1975) Geothermometry in sapphirine granulite: an evaluation of two-feldspar and pyroxene methods, (Abstr.). *Trans. Am. Geophys. Union.* **56**, 446.

THOMPSON, J. B. AND D. R. WALDBAUM (1969) Mixing properties of sanidine crystalline solutions: III. Calculations based on two phase data. *Am. Mineral.* **54**, 811–838.

TUTTLE, O. F. AND N. L. BOWEN (1958) Origin of granite in light of experimental studies in the system $NaAlSi_3O_8$–$KAlSi_3O_8$–

SiO$_2$–H$_2$O. *Geol. Soc. Am. Mem.* No. **74.** 153 p.

WALDBAUM, D. R. AND J. B. THOMPSON (1969) Mixing properties of sanidine crystalline solutions: IV. Phase diagrams from equations of state. *Am. Mineral.* **54,** 1274–1298.

WHITNEY, J. A. (1975) The effects of pressure, temperature, and X_{H_2O} on phase assemblage in four synthetic rock compositions. *J. Geol.,* **83,** 1–32.

———, J. C. STOMER, JR. AND R. L. SMITH (1975) Feldspar thermal histories for three post-metamorphic granites from the Georgia Piedmont (Abs). *Geol. Soc. Am. Abstr. with Program,* **7,** 549.

WONES, D. R. (1972) Stability of biotite: a reply. *Am. Mineral.* **57,** 316–317.

——— AND H. P. EUGSTER (1965) Stability of biotite: experiment, theory, and application. *Am. Mineral.* **50,** 1228–1272.